Autoreactive B cells in rheumatoid arthritis

Kristyanto, H.

Chapter VI

Citrullinated antigen-acalabrutinib conjugates for targeting autoreactive B cells

Hendy Kristyanto[1@#], *Bing Liu*[2@], *Lianne Lelieveldt*[3], *Theresa Kissel*[1], *Kimberly M. Bonger*[3], *Hans U. Scherer*[1], *Mario van der Stelt*[2], *Rene E.M. Toes*[1]

[1] *Department of Rheumatology, Leiden University Medical Center, the Netherlands*
[2] *Molecular Physiology Group, Leiden Institute of Chemistry, Leiden University, the Netherlands*
[3] *Department of Synthetic Organic Chemistry and Biomolecular Chemistry, Radboud University, Nijmegen, the Netherlands*
[@] *Hendy Kristyanto and Bing Liu contributed equally*

[#] *Hendy Kristyanto was responsible for the in vitro tests and immunology discussion described in the chapter*

Abstract

B cells require intact B cell receptor (BCR) signalling for their survival and activation. Bruton's tyrosine kinase (Btk) is a crucial part of the signalling pathway and has been targeted for the treatment of B cell lymphomas using small molecule inhibitors. In rheumatoid arthritis (RA), autoreactive B cells expressing and producing anti-citrullinated protein antibodies (ACPA) may play central roles in the pathogenesis of the disease. Most ACPA-expressing B cells display the phenotype of memory B cells that have recently been stimulated by antigen and T cells. In line, B cells from RA patients show enhanced expression of Btk and phospho-Btk. Therefore, suppression of BCR signalling by means of Btk inhibition, and in particular the specific targeting of autoreactive B cells, may serve as a potential therapeutic strategy for RA. Here, we synthesized the second generation Btk inhibitor Acalabrutinib and conjugated it with cyclic citrullinated peptides (CCP). The antigen-Acalabrutinib conjugate was able to suppress the viability of immortalized, ACPA-expressing B cells but not of control tetanus-toxoid specific B cells in a dose and treatment-duration dependent manner. This selective effect of the CCP-acalabrutinib conjugates could not be recapitulated by ten times more concentrated acalabrutinib or the combination of free CCP and free Acalabrutinib. To study the extent of Btk inhibition by these molecules, a competitive activity-based protein profiling assay for Btk was developed. This assay showed that the CCP-Acalabrutinib conjugates failed to inhibit Btk. In addition, calcium flux experiments also suggested that the conjugates did not inhibit BCR signalling. At present, these findings indicate that CCP-Acalabrutinib conjugates selectively inhibit the viability of ACPA-expressing B cells independent of Btk and BCR signalling inhibition. This possible off-target effect needs further elucidation.

Chapter VI

Introduction

Rheumatoid arthritis (RA) is a chronic autoimmune disease that causes debilitating joint pain and joint deformation. In the majority of RA patients, autoreactive anti-citrullinated protein antibodies (ACPA) can be detected years before the onset of disease and prognosticate progressive joint destruction in established disease. Previously, we showed that ACPA-expressing B cells in RA may exert functions relevant to disease pathogenesis by strongly expressing immune co-stimulatory molecules and by producing pro-inflammatory cytokines.[1] These cells also overexpress CD19, a plasma membrane protein which lowers the threshold of B cell receptor (BCR) signalling by amplifying and prolonging Bruton's tyrosine kinase (Btk) activation.[2] CD19 overexpression-induced BCR signalling enhancement promotes the loss of tolerance towards self-antigens and induces the formation of autoantibodies in mouse models.[3,4] Btk protein and its phosphorylated form are elevated in the total B cell population of ACPA-positive RA patients, if compared to B cells of ACPA-negative patients.[5] Moreover, inhibition of Btk reduces inflammatory responses and histological damage in murine models of RA.[6,7] These findings illustrate that Btk is a promising target to inhibit autoreactive B cells in RA.

Antigen binding to the BCR causes the clustering of CD79A/B which triggers the activation of kinases Lyn and Syk. In turn, Lyn and Syk phosphorylate CD79A and B, thereby commencing the formation of a BCR signalosome. In this signalling compartment, many adaptor proteins and other kinases such as Btk and Syk are recruited and activated, leading to amplification and propagation of downstream signals. Once phosphorylated, Btk and Syk phosphorylate phospholipase C-γ2 (PLC-γ2) which cleaves phosphatidyl-inositol-4,5-biphosphate (PIP2) into diacylglycerol (DAG) and inositol-1,4,5-triphosphate (IP3). Subsequently, DAG and IP3 activate protein kinase C and induce calcium influx which are crucial for B cell activation and survival.[8]

The first generation Btk inhibitor Ibrutinib has been introduced for clinical use to treat chronic lymphocytic leukemia (CLL).[9] Ibrutinib inhibits not only Btk but also other kinases which contributes to the manifestation of side effects including bleeding, hypertension and atrial fibrillation.[10-12] To overcome the limitations of the first generation Btk inhibitor, second generation Btk inhibitors such as Acalabrutinib have been developed and are currently being used to treat CLL patients who are intolerant to ibrutinib.[13] Acalabrutinib is a highly selective Btk inhibitor which binds to the active site of the kinase covalently and therefore

inhibits the protein irreversibly.[14] Despite improved selectivity for Btk, up to 16% of Waldenström macroglobulinemia patients treated with Acalabrutinib developed grade 3-4 adverse events including neutropenia, pneumonia, bleeding and sepsis.[15] Therefore, strategies to increase the safety profile and efficacy of Acalabrutinib are necessary for treating autoimmune diseases and may be of value to facilitate clinical use of these and other potent kinase inhibitors.

In this chapter, we explored the use of an antigen-directed immunotherapy strategy to selectively deliver Acalabrutinib to ACPA-expressing B cells. To examine the inhibitory activity of Acalabrutinib and of cyclic citrullinated peptide (CCP)-conjugated Acalabrutinib, an activity-based protein profiling (ABPP) assay for Btk was developed. Complete inhibition of Btk by Acalabrutinib in immortalized, ACPA-expressing B cells affected anti-IgG-nduced proliferation but not the viability of these cells. Surprisingly, however, the CCP-Acalabrutinib conjugates inhibited ACPA-expressing B cell survival in a dose and time dependent manner, despite an apparent failure to inhibit BCR signalling in these cells. Moreover, this effect was not observed in immortalized, tetanus-toxoid specific B cells. These findings suggested that the CCP-Acalabrutinib conjugates may have a selective inhibition on immortalized, ACPA-expressing B cells which is independent of BCR signalling inhibition.

Materials and Methods

Compounds synthesis

General compound synthesis, purification and analysis methods: All solvents and reagents were obtained commercially and used as received unless stated otherwise. Reactions were executed at room temperature unless stated otherwise. Moisture sensitive reactions were performed under argon atmosphere. Water was removed from starting compounds by repetitive co-evaporation with toluene. Solvents were removed by evaporation under reduced pressure. DCM, DMF, and THF were dried over activated 4Å molecular sieves for at least 12 hours before use. Compounds were visualized during TLC analyses by UV (254 nm), and with the staining solutions: aqueous solution of $KMnO_4$ (5 g/L) and K_2CO_3 (25 g/L). Visualization of hemiacetals and glycosides was achieved by spraying with a solution of 20% H_2SO_4 in ethanol followed by charring at ≈ 200˚C. Column chromatography purification was performed on silica gel (40-63 μm). ^1H and ^{13}C-APT NMR spectra were recorded

on a Bruker AV 400 (400/100 MHz) or Bruker 600 (600/150 MHz) spectrometer in $CDCl_3$, MeOD or D_2O. Chemical shifts are given in ppm (δ) relative to TMS as internal standard (^1H NMR in $CDCl_3$) or the signal of the deuterated solvent[16]. Coupling constants (*J*) are given in Hz. High resolution mass spectra were recorded by direct injection (2 μL of a 2μM solution in water/acetonitrile/*tert*-butanol 1:1:1 v/v/v) on a mass spectrometer (Thermo Finnigan LTQ Orbitrap) equipped with an electrospray ion source with resolution R = 60000 at *m/z* 400 (mass range *m/z* = 150-2000). IR spectra were recorded on a Shimadzu FTIR-8300 and are reported in cm^{-1}. Optical rotation were measured on an automatic polarimeter of sodium D-line, at λ =589 nm. Size-exclusion purifications were performed on an ÄKTA-explorer, column size d = 26 mm, l = 60 mm, mobile phase NH_4HCO_3 (0.15 M) in H_2O, flow 1.5 mL/min. HPLC Purification were performed on a Prep LCMS, Gemini from Phenomenex B.V. (C-18, 110 Å, 5 μm, 19 × 150 mm column).

Compounds:

(S)-4-(8-Amino-3-(pyrrolidin-2-yl)imidazo[1,5-a]pyrazin-1-yl)-N-(pyridin-2-yl)benzamide (P007)

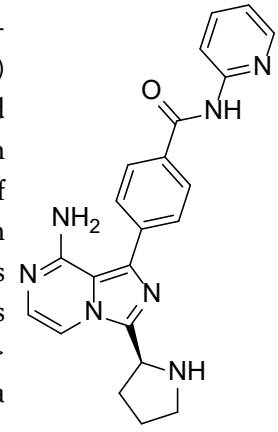

To a solution of (S)-benzyl 2-(8-amino-1-(4-(pyridin-2-ylcarbamoyl)phenyl)imidazo[1,5-a]pyrazin-3-yl) pyrrolidine-1-carboxylate (0.33g, 0.62 mol, synthesized as reported in WO 2013/010868, A1, Page/Page column 32) in methanol (10 mL) was added a catalytic amount of $Pd(OH)_2$. The reaction mixture was stirred with hydrogen balloon overnight at room temperature. The mixture was filtrated on celite and concentrated. The crude product was purified using silica gel column (DCM/MeOH = 20/1 -> 5:1 v/v) to afford **P007** (0.20 g, 0.50 mmol, yield 83%) as a yellow solid.

^1H NMR (400 MHz, MeOD) δ 8.36 (ddd, *J* = 4.9, 2.0, 0.9 Hz, 1H), 8.23 (dt, *J* = 8.4, 1.0 Hz, 1H), 8.14 – 8.04 (m, 2H), 7.89 – 7.77 (m, 3H), 7.67 (d, *J* = 5.1 Hz, 1H), 7.16 (ddd, *J* = 7.4, 5.0, 1.0 Hz, 1H), 7.09 (d, *J* = 5.1 Hz, 1H), 5.49 (s, 1H), 4.86 (t, *J* = 7.5 Hz, 1H), 3.38 – 3.26 (m, 1H), 3.18 (ddd, *J* = 11.0, 7.9, 5.9 Hz, 1H), 2.49 – 2.28 (m, 2H), 2.23 – 1.97 (m, 2H). ^{13}C NMR (101 MHz, MeOD) δ 167.9, 153.4, 153.2, 149.2, 141.8, 139.6, 139.1, 136.0, 135.2, 130.9, 129.2, 128.8, 121.3, 116.3, 116.3, 108.0, 55.0, 47.5, 31.1, 26.4.

(S)-4-(8-amino-3-(1-but-2-ynoylpyrrolidin-2-yl)imidazo[1,5-a]pyrazin-1-yl)-N-(pyradin-2-yl)benzamide (Acalabrutinib)

To a suspension of **P007** (63.4 mg, 0.17 mmol), 2-butynoic acid (15 mg, 0.18 mmol) and TEA (0.11 mL, 0.82 mmol) in DCM (4 mL), was added HATU (65 mg, 0.17 mmol). The reaction mixture was kept stirred at r.t. overnight. The reaction mixture was washed with water (5 mL), the aqueous layer was re-extracted with DCM (2 × 5 mL). the combined organic layer was dried over Na_2SO_4 anh., filtrated and concentrated. The residue was purified with HPLC to get **Acalabrutinib** (14 mg, 0.03 mmol, yield 18%). R_f = 0.43 (EtOAc: MeOH = 3:1).

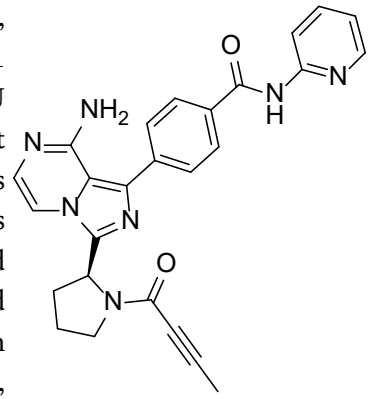

^{1}H NMR (400 MHz, MeOD) δ 8.54 – 8.19 (m, 2H), 8.14 – 8.05 (m, 2H), 7.91 – 7.62 (m, 4H), 7.28 – 6.93 (m, 2H), 5.80 – 5.38 (m, 1H), 4.20 – 3.59 (m, 2H), 2.72 – 2.04 (m, 4H), 2.02 (s, 2H), 1.63 (s, 1H). ^{13}C NMR (100 MHz, MeOD) δ 168.0, 155.1, 153.2, 143.5, 142.6, 139.6, 139.0, 136.2, 135.3, 131.1, 129.2, 128.4, 121.3, 116.3, 115.5, 108.3, 90.8, 74.5, 53.5, 50.1, 32.6, 25.4, 3.3. LC-MS analysis: Rt 4.70 min (linear gradient 0-90%) acetonitrile in H_2O, 0.1% TFA, 12.5 min.

tert-Butyl 4-(2-hydroxyethyl)piperazine-1-carboxylate (BL020)

To a solution of 2-(piperazin-1-yl) ethanol (2.60 g, 20 mmol) and Boc_2O (5.0 g, 22 mmol) in methanol (30 mL) was added Et_3N (4.2 mL, 30 mmol). The mixture was stirred at room temperature for 3 hours. The solvent was removed in vacuo. The residue was diluted with water and extracted with EtOAc (3 x 40 mL). the combined organic layer were washed with brine and dried over Na_2SO_4. After filtration and concentration, the product was obtained as light yellow oil (4.58 g, yield 99%).

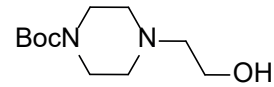

^{1}H NMR (400 MHz, MeOD) δ 3.68 (t, *J* = 5.9 Hz, 2H, H_2-1), 3.44 (t, *J* = 5.1 Hz, 4H, H_2-4, H_2-4'), 2.53 (t, *J* = 5.9 Hz, 2H, H_2-2), 2.49 – 2.42 (m, 4H, H_2-3, H_2-3'), 1.46 (s, 9H, 3 × CH_3). ^{13}C NMR (100 MHz, MeOD) δ 156.4 (C-5), 81.2 (C-6), 61.3 (C-2), 59.8 (C-1), 54.3 (C-3), 28.6 (3 × CH_3).

tert-Butyl 4-(2-chloroethyl)piperazine-1-carboxylate (BL022)

BL20 (4.60 g, 20 mmol) was dissolved in DCM (100 mL), Et_3N (6.06 g, 60 mmol), DMAP (244 mg, 2.0 mmol) and p-toluenesulfonyl chloride (5.74 g, 30 mmol) was

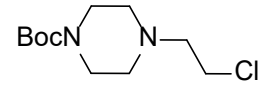

added and the reaction mixture stirred at room temperature for 16 hours. Sodium bicarbonate aqueous solution (saturated, 100 mL) was added to the reaction mixture, and aqueous phase was extracted with DCM (2 x 50 mL), and the organic phase combined was washed with saturated brine (2 x 30 mL). The organic layer was dried over Na_2SO_4, filterated and concentrated. The residue was purified by column chromatography on silica gel column using eluent system 10% methanol in EtOAc to give **BL022** as oil (4.43 g, yield 69%).

^{1}H NMR (400 MHz, $CDCl_3$) δ 3.59 (t, *J* = 7.0 Hz, 2H, H_2-1), 3.48 – 3.36 (m, 4H, H_2-4, H_2-4'), 2.74 (t, J = 6.9 Hz, 2H, H_2-2), 2.46 (t, *J* = 5.0 Hz, 4H, H_2-3, H_2-3'), 1.46 (s, 9H, 3 × CH_3). ^{13}C NMR (101 MHz, $CDCl_3$) δ 154.8 (C-5), 79.8 (C_q-Boc), 59.9 (C-2), 53.0 (C-3, C-3'), 43.6 (C-4, C-4'), 40.9 (C-1), 28.5 (3 × CH_3).

tert-Butyl 4-(2-azidoethyl)piperazine-1-carboxylate (BL023)

To a mixture of **BL22** (1.0 g, 4.02 mmol) in DMF (10 mL) and H_2O (20 mL) was added sodium azide (0.78 g, 12.06 mmol). The reaction mixture was stirred overnight at 70°C.

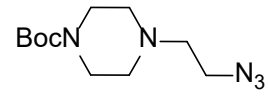

The reaction mixture was extracted with DCM (3 x 30 mL). The combined organic layer was washed with water and brine. The organic layer were dried over Na_2SO_4, filtered and concentrated not yet to 100% dryness. The crude product was used derectly in the next step.

^{1}H NMR (400 MHz, $CDCl_3$) δ 3.45 (t, *J* = 5.1 Hz, 4H, H_2-4, H_2-4'), 3.35 (t, *J* = 6.0 Hz, 2H, H_2-1), 2.61 (td, *J* = 6.0, 1.2 Hz, 2H, H_2-2), 2.45 (t, *J* = 5.0 Hz, 4H, H_2-3, H_2-3'), 1.46 (s, 9H, 3 × CH_3). ^{13}C NMR (100 MHz, $CDCl_3$) δ 154.8 (C-5), 79.8 (C_q-Boc), 57.3 (C-1), 53.0 (C-3, C-3'), 48.2 (C-2), 43.9 (C-4, C-4'), 28.5 (3 × CH_3).

2-(Piperazin-1-yl)-1-azidoethane (BL024)

To a 2M solution of **BL024** in DCM (2 mL) was added TFA (2 mL). The reaction mixture was kept stirred at room temperature for 1 hour. The reaction mixture was quenched with aqueous K_2CO_3 (5 mL, 2M). The reaction mixture was extracted with DCM (3 x 20 mL), the combined organic layres were washed with brine, dried over Na_2SO_4, filtrated and concentrated (not to 100% dry). The crude product was used in next step without further purification.

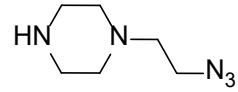

^{1}H NMR (400 MHz, MeOD) δ 3.42 (t, *J* = 6.2 Hz, 2H, H_2-1), 2.90 – 2.84 (m, 4H, H_2-3, H_2-3'), 2.60 – 2.55 (m, 2H, H_2-2), 2.56 – 2.46 (m, 4H, H_2-4, H_2-4').^{13}C

NMR (101 MHz, MeOD) δ 58.4 (C-2), 54.5 (C-4, C-4'), 48.9 (C-1), 45.9 (C-3, C-3').

1-(2-Azidoethyl)-4-(but-3-yn-1-yl)piperazine (BL025)

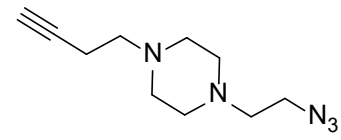

To a solution 1-(2-azidoethyl)piperazine (0.31 g, 2.00 mmol) and 4-bromobut-1-yne (0.19 mL, 1.63 mmol) in acetonitrile (10 mL), were added K_2CO_3 (0.83 g, 6.00 mmol) and KI (0.33 g, 1.99 mmol). The mixture was kept stirred at r.t overnight. After a filtration, the filtrate was concentrated on a rotary evaporator. The residue was purified with silica gel column chromatography (5% MeOH and 1% TEA in EtOAc) to give **BL025** (0.10g, 0.48 mmol, yield 24%) as thick yellow oil.

^{1}H NMR (400 MHz, Chloroform-d) δ 3.44 – 3.37 (m, 2H, H_2-1), 2.79 (t, *J* = 7.4 Hz, 2H, H_2-5), 2.76 (br s, 8H, H_2-3, H_2-4, H_2-3', H_2-4'), 2.71 – 2.65 (m, 2H, H_2-2), 2.56 (td, *J* = 7.4, 2.7 Hz, 2H, H_2-6), 2.04 (t, *J* = 2.7 Hz, 1H, H-8). ^{13}C NMR (100 MHz, $CDCl_3$) δ 70.1 (C-7), 56.8 (C-2), 56.5 (C-5), 52.5 (C-4, C-4'), 52.0 (C-3, C-3'), 48.0 (C-1), 21.1 (C-8), 16.3 (C-6). IR/cm^{-1}: 3441, 2943, 2819, 2098, 1660, 1449, 1286, 1156, 1007, 937.

5-(4-(2-Azidoethyl)piperazin-1-yl)pent-2-ynoic acid (BL026)

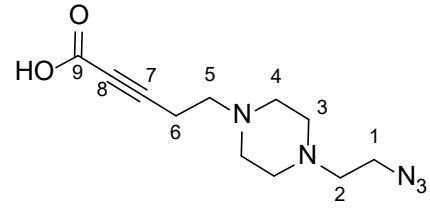

n-BuLi (1.6 M in hexane, 0.35 mL, 0.56 mmol) was added to a solution of **BL025** (75 mg, 0.36 mmol) in THF (2 mL) at -78°C. After 1 hour, carbon dioxide (dried with a drying tower, filling: 4A molecular sieves, $CaCO_3$ and CuSO4) was bubbled for 2 hours into the solution. The reaction was then quenched by adding water dropwise. The mixture was warmed to r.t., and washed with EtOAc (2 × 3 mL), and the aqueous phase was concentrated. The residue was dissolved in MeOH, the not dissolved LiOH was removed by filtration. The volatile was evaporated to gain BL026 (32 mg, 0.13 mmol, yield 35%), which was used in the next step without further purification. R_f = 0.14 (EtOAc: MeOH = 3:1).

^{1}H NMR (400 MHz, Methanol-d_4) δ 3.41 (dd, *J* = 6.6, 5.4 Hz, 2H, H_2-6), 2.70 (dd, *J* = 8.0, 6.9 Hz, 2H, H_2-2), 2.66 (br s, 8H, H_2-3, H_2-4, H_2-3', H_2-4'), 2.63 (dd, *J* = 6.6, 5.4 Hz, 2H, H_2-5), 2.52 (dd, *J* = 8.0, 6.9 Hz, 2H, H_2-1). ^{13}C NMR (101 MHz, MeOD) δ 161.5 (C-9), 80.5 (C-8), 79.4 (C-7), 57.8 (C-2), 57.3 (C-5), 53.4, 53.3 (C-3, C-4, C-3', C-4'), 49.0 (C-6), 17.0 (C-1). IR/cm^{-1}: 3356, 2948, 2822,

2235, 2098, 1574, 1366, 1301, 1156, 1009.

(S)-4-(8-Amino-3-(1-(5-(4-(2-azidoethyl)piperazin-1-yl)pent-2-ynoyl) pyrrolidin-2-yl)imidazo[1,5-a]pyrazin-1-yl)-N-(pyridin-2-yl)benzamide (P010)

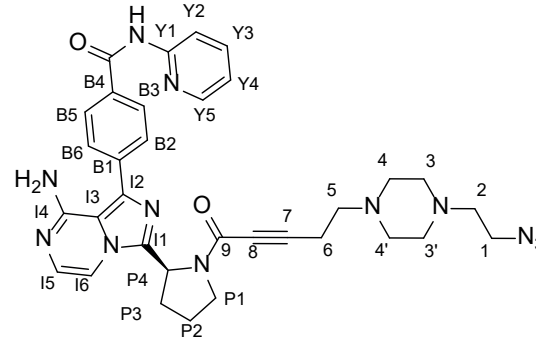

To a mixture of HATU (30 mg, 0.079 mmol), **BL026** (20 mg, 0.079 mmol) in DCM (5 mL) was added **P007** (31.7 mg, 0.079 mmol) and Et_3N (5.5 µL, 0.04 mmol). The reaction mixture was stirred overnight at room temperature. The mixture was washed with brine, dried over Na_2SO_4, filtrated and concentrated. The crude product was purified with silica gel chromatography, with eluent system 2% - 5% methanol in DCM to give **P010** 36 mg, yield 71%.

^{1}H NMR (400 MHz, MeOD) δ 8.41 – 8.21 (m, 2H, H_2-Y), 8.19 – 8.06 (m, 2H, H_2-B), 7.91 – 7.67 (m, 4H, H_1-Y, H_2-B, H_1-I), 7.24 – 7.03 (m, 2H, H_1-Y, H_1-C), 5.98 – 5.22 (m, 1H, H-P4), 4.10 – 3.65 (m, 2H, H_2-P1), 3.41 – 3.33 (m, 2H, H_2-6), 2.75 – 1.98 (m, 18H, H_2-1, H_2-2, H_2-3, H_2-4, H_2-3', H_2-4', H_2-5, H_2-P2, H_2-P3). ^{13}C NMR (100 MHz, MeOD) δ 172.3 (C=O), 167.9 (C-I4), 154.9 (C-Y1), 153.3 (C-I1), 153.2 (C-9), 149.2 (C-Y), 143.5 (C_q-B), 142.6 (C_q-B),139.6 (C_q-I), 138.8, 131.0, 129.2 (C-B), 128.4 (C-B), 121.4, 116.3, 107.5, 92.2, 75.9, 58.0, 56.9, 56.3, 50.3, 47.7, 33.4, 32.6, 25.4, 24.3, 17.4. IR/cm^{-1}: 3313, 2948, 2817, 2239, 2102, 1607, 1518, 1430, 1305. LC-MS analysis: Rt 4.39 min (linear gradient 0-90%) acetonitrile in H_2O, 0.1% TFA, 12.5 min.

ert-butyl (2-(4-(but-3-yn-1-yl)piperazin-1-yl)ethyl)carbamate (BL017)

To a solution of tert-butyl (2-(piperazin-1-yl)ethyl)carbamate (0.24 g, 1.03 mmol) and 4-bromobut-1-yne (0.1 mL, 1.06 mmol) in acetonitrile (5 mL), was added K_2CO_3 (0.43 g, 3.09 mmol) and KI (0.17 g, 1.03 mmol). The mixture was kept stirred at r.t overnight. After a filtration, the filtrate concentrated on a rotary evaporator. The residue was purified with silica gel column chromatography (5% MeOH and 1% TEA in EtOAc) to get **BL017** (0.11g, 0.39 mmol, yield 38%) as thick yellow oil. R_f = 0.38 (EtOAc: MeOH = 3:1, with 1% TEA).

^{1}H NMR (400 MHz, MeOD) δ 3.25 (t, *J* = 6.6 Hz, 2H, H_2-1), 2.73 (t, *J* = 7.5 Hz, 2H, H_2-5), 2.66 (t, *J* = 6.6 Hz, 2H, H_2-2), 2.46 (ddd, *J* = 8.1, 7.0, 2.7 Hz, 2H,

H_2-6), 2.34 (t, *J* = 2.7 Hz, 1H, H-8), 1.44 (s, 9H, 3 × CH_3). ^{13}C NMR (100 MHz, MeOD) δ 158.4 (C=O), 82.2 (C-7), 80.2 (C_q), 71.1 (C-8), 58.2 (C-2), 57.4 (C-5), 53.1, 52.8 (C-3, C-4, C-3', C-4'), 37.8 (C-1), 28.7 (3 × CH_3), 16.9 (C-6). IR/cm^{-1}: 2941, 2815, 2490, 2362, 1694, 1412, 1247, 1154.

5-(4-(2-((tert-butoxycarbonyl)amino)ethyl)piperazin-1-yl)pent-2-ynoic acid (BL016)

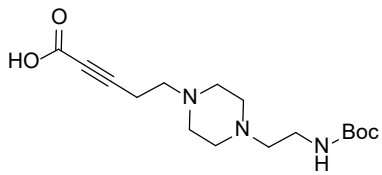

n-BuLi (1.6 M in hexane, 1.7 mL, 2.72 mmol) was added to a solution of **BL017** (0.61 g, 2.14 mmol) in THF (13 mL) at -78°C. After 1 hour activation, dried carbon dioxide was bubbled for 2 hours into the solution. The reaction was then quenched by adding water dropwise. The mixture was warmed to r.t., and washed with EtOAc (2 × 10 mL). The aqueous phase was concentrated. The residue **BL016** (0.48 g, 1.50 mmol, yield 70%) was used in the next step without further purification. R_f = 0.28 (EtOAc: MeOH = 1:1).

VI

^{1}H NMR (400 MHz, MeOD) δ 3.18 (t, *J* = 6.8 Hz, 2H, H_2-6), 2.61 (ddd, *J* = 8.0, 6.9, 0.9 Hz, 2H, H_2-5), 2.56 (s, 8H, H_2-3, H_2-4, H_2-3', H_2-4'), 2.51 – 2.44 (m, 2H, H_2-1), 2.45 (t, *J* = 6.8 Hz, 2H, H_2-2), 1.43 (s, 9H, 3 × CH_3). ^{13}C NMR (100 MHz, MeOD) δ 161.7, 158.4 (2 × C=O), 80.3 (C-8), 79.7 (C-7), 58.6 (C-2), 57.7 (C-5), 53.8, 53.5 (C-3, C-4, C-3', C-4'), 38.4 (C-6), 28.8 (3 × CH_3), 17.3 (C-1).

tert-butyl (S)-(2-(4-(5-(2-(8-amino-1-(4-(pyridin-2-ylcarbamoyl)phenyl imidazo[1,5-a]pyrazin-3-yl)pyrrolidin-1-yl)-5-oxopent-3-yn-1-yl)piperazin-1-yl)ethyl)carbamate (P009)

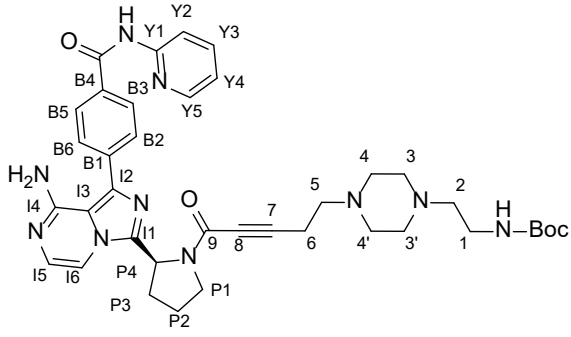

To a solution of P007 (50.0 mg, 0.13 mmol), BL016 (41.2 mg, 0.13 mmol) and TEA (0.009 mL, 0.06 mmol) in DCM (8 mL), was added HATU (42.7 mg, 0.11 mmol). The mixture was kept stirred at r.t. overnight. After washed with water (10 mL), the aqueous layer was re-extracted with DCM (2 × 8 mL). the combined organic layer was dried over Na_2SO_4 anh., filtrated and concentrated. The residue was purified with silica gel column chromatography (5% MeOH in DCM) to get P009 (29 mg, 0.041 mmol, yield 32 %). R_f = 0.44 (DCM: MeOH = 10:1).

^{1}H NMR (400 MHz, $CDCl_3$) δ 8.61 – 8.04 (m, 4H), 7.86 – 7.59 (m, 3H), 7.27 – 6.85 (m, 2H), 5.67 – 5.37 (m, 1H), 3.96 – 3.82 (m, 2H), 3.80 – 3.64 (m, 12H), 2.78 – 1.75 (m, 10H), 1.45 – 1.24 (m, 9H). ^{13}C NMR (100 MHz, $CDCl_3$) δ 177.0, 172.4, 167.9, 153.4, 153.2, 149.2, 143.5, 139.6, 139.1, 135.4, 131.1, 129.2, 128.3, 121.4, 116.3, 108.2, 68.9, 53.9, 32.2, 26.5, 25.7, 22.5. IR/cm^{-1}: 3202, 2342, 2135, 1610, 1521, 1432, 1306. LC-MS analysis: Rt 4.72 min (linear gradient 0-90%) acetonitrile in H_2O, 0.1% TFA, 12.5 min).

(S)-4-(8-amino-3-(1-(5-(4-(2-aminoethyl)piperazin-1-yl)pent-2-ynoyl) pyrrolidin-2-yl)imidazo[1,5-a]pyrazin-1-yl)-N-(pyridin-2-yl)benzamide (P011)

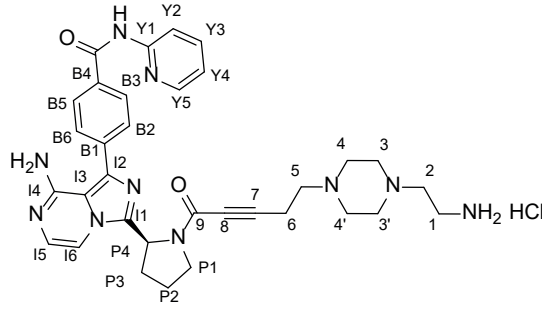

To a solution of **P009** (60 mg, 0.085 mmol) in methanol (5 mL), was added HCl in dioxane (4N, 3 mL, 12 mmol). The reaction mixture was kept stirred at r.t. overnight. Volatile was removed in vacuum, to get **P011** (48 mg, 0.074 mmol, yield 87%) in the residue as a HCl salt. The crude product was used in next step without further purification.

1-(6-((2-(4-(5-((S)-2-(8-amino-1-(4-(pyridin-2-ylcarbamoyl)phenyl) imidazo[1,5-a]pyrazin-3-yl)pyrrolidin-1-yl)-5-oxopent-3-yn-1-yl)piperazin-1-yl)ethyl)amino)-6-oxohexyl)-3,3-dimethyl-2-((1E,3E)-5-((E)-1,3,3-trimethylindolin-2-ylidene)penta-1,3-dien-1-yl)-3H-indol-1-ium (P015)

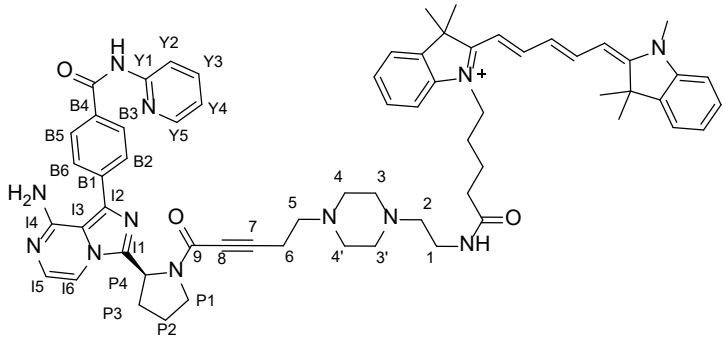

Cy5-OSu (12 mg, 0.019 mmol) was added to a solution of P011 (12 mg, 0.020 mmol) and DiPEA (0.015 mL, 0.086 mmol) in DMF (1 mL). The reaction mixture was kept stirred at r.t. overnight. After removing DMF on a rotary evaporator, the residue was purified using HPLC to get P015 (2.8 mg, 0.0025 mmol, yield 12.8%). Mass found:1758.60.

P010+DBCO-containing peptide

The synthesis of cyclic citrullinated peptide followed the published protocol.[17] Moreover, DBCO-containing cyclic citrullinated peptide synthesis was previously described.[18] The norleucine peptide control was synthesized by replacing one citrulline amino acid with norleucine. **P010** (0.77 mg, 1200 nmol, 2eq) and peptide (1.66 mg, 611 nmol, 1eq) was dissolved in 0.6 mL MilliQ and 0.1 mL methanol. This solution was left at room temperature overnight. After LC-MS monitored no peptide left, the reaction mixture was purified by HPLC: Rt 4.18 min (linear gradient 0-90%) acetonitrile in H_2O, 0.1% TFA, 12.5 min, Mass found:1151.00 (3 charged) and 1726.33 (2 charged).

Cell culture and viability assay

BCL-6 and BCL-XL-immortalized primary ACPA-positive and tetanus-specific B cell lines were previously described.[1] The cells were preconditioned with recombinant human CD40 ligand (Biolegend) for three days prior to the experiment to get rid of the remaining of CD40L-expressing feeder cells. To identify which dose could inhibit ACPA-positive B cell viability, 50,000 ACPA-positive and tetanus-specific B cells were cultured in 100 µL MDM medium supplemented with 8% fetal calf serum, 100 U/ml penicillin/streptomycin and 2 mM Glutamax in U-bottomed 96 well plate. Into the cell culture, final concentrations of 25 nM, 50 nM, 100 nM, 400 nM and 800 nM of Acalabrutinib, CCP-Acalabrutinib conjugate and CNleP-Acalabrutinib conjugate was added on day 1, 2, 3 and 4. Drug-naïve cells and 33% DMSO-culled cell culture were taken along as controls. Additionally, goat anti-human IgG F(ab')2 fragment (Jackson's laboratory) was added into the cell culture on day 2, 3 and 4 to induce BCR activation. On day 5, XTT viability assay (Merck) was conducted according to manufacturer's instruction.[17] Percentage of viable cells was normalized with the colorimetric result of anti-IgG- and drug-naïve cell culture. Each condition was done in three technical replicates.

To identify the effect of treatment duration on cell's viability, 50,000 immortalized ACPA-positive and tetanus-specific B cells were cultured as above. Three conditions were experimented, namely 2, 3 and 4 days of treatment duration. Into the cell culture, a final concentration of 800 nM of Acalabrutinib, CCP-Acalabrutinib and CNleP-Acalabrutinib was added on day 1 and 2; day 1, 2 and 3; and day 1, 2, 3 and 4. Additionally, anti-IgG F(ab') 2 fragment was added on day 2; day 2 and 3; and day 2, 3 and 4 respectively. On day 3, 4 and 5 the XTT viability assay was conducted as above.

To identify the effect of high concentration of Acalabrutinib on the immortalized B cells, 50,000 cells were cultured in the presence of 800 nM CCP-Acalabrutinib and 800 nM CNleP-Acalabrutinib. Moreover 800 nM, 4 μM and 8 μM of Acalabrutinib was added on day 1 until 6. In addition, to test the effect of peptide addition to Acalabrutinib function, 800 nM of free CCP, CNleP, a combination of free CCP + Acalabrutinib and a combination of free CNleP + Acalabrutinib were added to cell culture for six days. On day 7 XTT viability assay was conducted as above.

Gel-based activity-based protein profiling (ABPP) assay for Btk

To assess the occupancy of Btk by Acalabrutinib and the peptide conjugates, 50,000 immortalized ACPA-positive B cells were cultured in the presence of 5 nM, 50 nM, 100 nM Acalabrutinib, a combination of free CCP and Acalabrutinib, CCP-Acalabrutinib conjugate and CNleP-Acalabrutinib conjugate. After two days of incubation, the cells were centrifuged and washed with cold PBS (pH 7.4) before being lysed with 20 μL lysis buffer and frozen at -80˚C. The cell lysate was thawed and added 0.5 uL **P015** (a final concentration of 2 μM) at 37˚C for 15 minutes which bound to the unoccupied Btk. The probe-labelled samples were then loaded into 1D SDS-PAGE and visualized by in-gel fluorescence scanning.

Calcium flux assay

To assess the extent of BCR signalling inhibition by Acalabrutinib and the peptide conjugates, 100,000 ACPA-expressing Ramos cell line were treated with 800 nM of Acalabrutinib, a combination of CCP + Acalabrutinib, CCP-Acalabrutinib conjugate and CNleP-Acalabrutinib conjugate for two days.[19] During flow cytometry measurement, the cells were treated with anti-IgG F(ab')2 fragment in the presence of Indo-1 calcium indicator (ThermoFisher). Indo-1 ratio of all conditions, indicating the relative extent of calcium flux, was represented.

Statistical analysis

Statistical analyses were performed using GraphPad Prism 9.3.1. The magnitude of difference in percentage of living cells following treatment with different compounds of various concentrations or different duration of treatment or on different cell lines was tested using two-way analysis of variance (ANOVA) followed by Tukey's honestly significant difference (Tukey HSD) *post-hoc* test. Specific information is provided in the figure legends.

Results

Synthesis of Acalabrutinib and of antigen-Acalabrutinib conjugates

Autoreactive B cells play central roles in the pathogenesis of RA. These cells display hyperactivated BCR signalling which may serve as a target for therapy.[20] One of the upstream signalling proteins in the BCR signalling pathway is Btk. Here, we first synthesized the second generation, highly specific Btk inhibitor Acalabrutinib (Figure 1A). To target ACPA-expressing B cells specifically, a cyclic citrullinated peptide (CCP) was conjugated to Acalabrutinib. To this end, a 5-(4-(2-Azidoethyl) piperazin-1-yl)pent-2-ynoic acid handle was synthesized and conjugated to Acalabrutinib (Figure 1B and C). Subsequently, DBCO-containing CCP was reacted to the azide-containing Acalabrutinib via a copper-free click reaction to yield the antigen-Acalabrutinib conjugate (Figure 1C). The antigen used, CCP, has previously been shown to be recognized by the majority of ACPA from RA patients and is well recognized by the immortalized, ACPA-expressing B cell line used in our studies.[17] As a control antigen, a norleucine-containing cyclic peptide (CNleP) was used. Citrulline results from the post-translational modification of arginine residues. Here, we chose CNleP instead of the arginine-containing control peptide CArgP, because like citrulline, norleucine is neutrally charged. Previous studies in our laboratory have shown that CArgP, unlike CCP and CNleP, shows non-specific binding to cell surfaces that can result in over-interpretation of background signals (data not shown). The remaining amino acid sequence of the cyclic peptide is the same for both CCP and CNleP.

Dose dependent, selective effects of the CCP-Acalabrutinib conjugate on immortalized, ACPA-expressing B cells

We next tested the effect of different concentrations of Acalabrutinib and of the antigen-Acalabrutinib conjugates on immortalized, ACPA-expressing B cells. Final concentrations of 0 nM, 25 nM, 50 nM, 100 nM, 200 nM, 400 nM and 800 nM of Acalabrutinib, CCP-Acalabrutinib (CCP-Aca) and CNleP-Acalabrutinib (CNleP-Aca) conjugates were added to immortalized ACPA-expressing B cells and to immortalized tetanus toxoid (TT)-specific B cells used as controls. Cultures were performed for four consecutive days. A BCR stimulant, anti-human IgG F(ab')2 antibody fragment, was concurrently added on days 2, 3 ,and 4. On day 5, cell viability was assessed using a XTT cell viability assay. As compared to cells that received neither the drug nor anti-IgG F(ab')2 antibody fragments (set to 100% living cells), drug naïve, anti-IgG-treated ACPA-expressing and tetanus-toxoid specific B cell

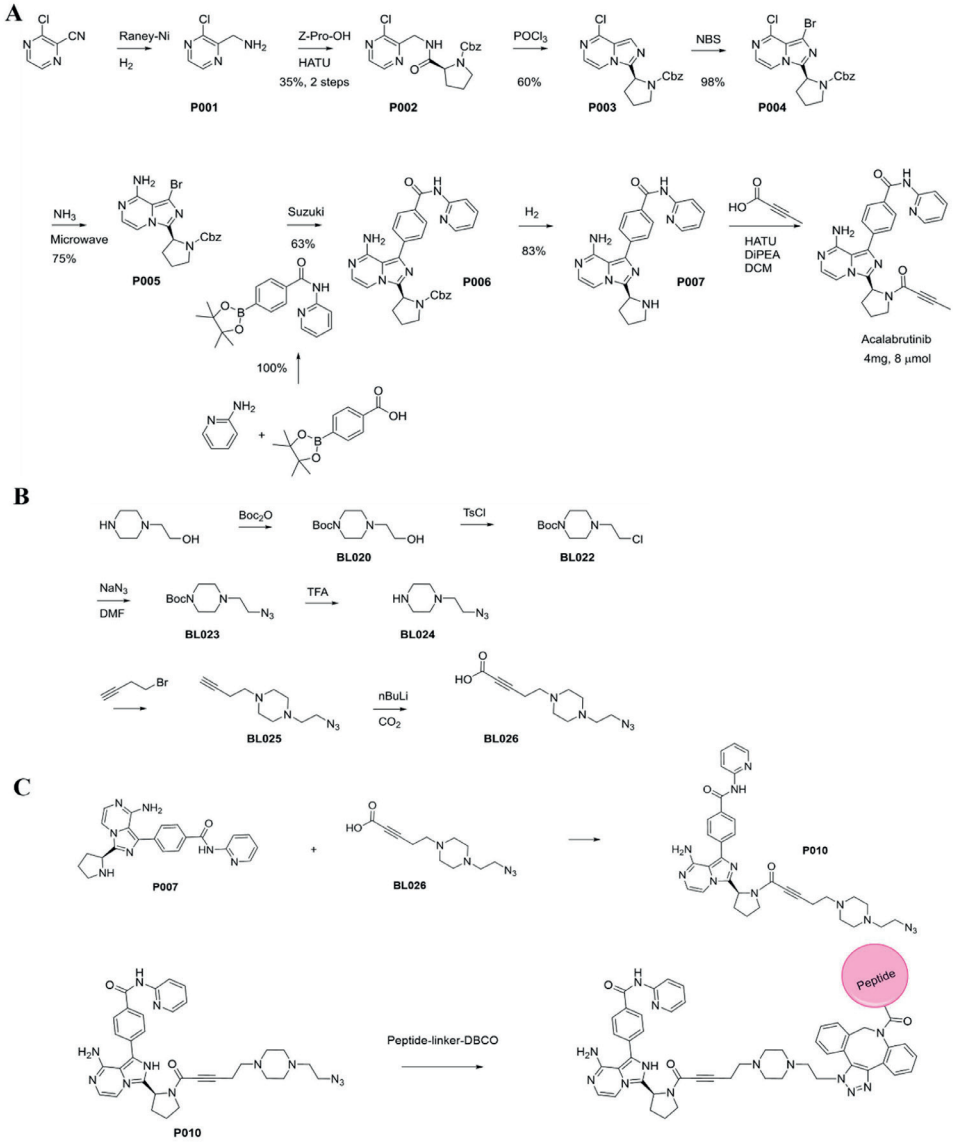

Figure 1. Synthesis of compounds. **A**) Synthesis of acalabrutinib, **B**) handle and **C**) antigen-Acalabrutinib conjugate

lines showed additional cell growth and/or proliferation (Figure 2A and B) during the five days of culture. Treatment with Acalabrutinib did not significantly reduce cell viability of both ACPA-expressing and TT-specific B cell lines (Figure 2A and B), suggesting that these cell lines may not require BCR signalling for their survival in the steady state, in-line with their immortalized phenotype. Remarkably, CCP-Aca, but not CNleP-Aca, inhibited the survival of immortalized, ACPA-expressing B cells in a dose dependent manner (Figure 2A). Statistical analysis using two-way

analysis of variance (ANOVA) followed by Tukey's honestly significant difference (HSD) test revealed that a statistically significant reduction of the percentage of living cells was observed following 200nM CCP-Aca treatment ($p \leq 0.01$). The percentage of living cells decreased further with higher doses (Figure 2A). This effect was not observed in the TT-specific control B cell line (Figure 2B). Together, these findings suggest that stimulation of the BCR by anti-IgG F(ab')2 fragments induces Btk-dependent proliferation, and indicate a selective, possibly cytotoxic effect of high doses of CCP-Acalabrutinib on anti-IgG F(ab')2 fragment-stimulated, ACPA-expressing B cells.

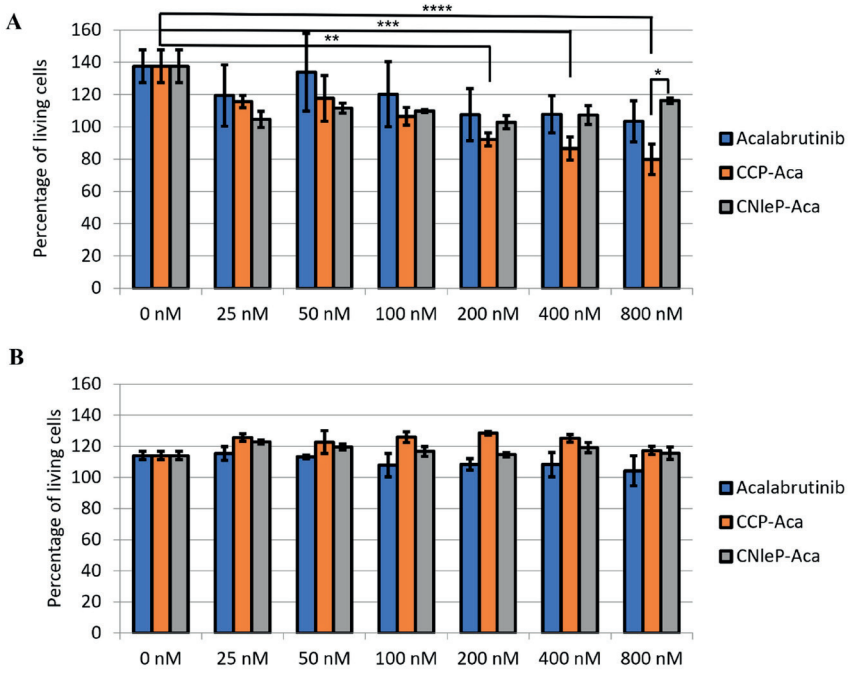

Figure 2. Selective reduction of ACPA-expressing B cells viability by CCP-acalabrutinib conjugates in dose-dependent manner. A) Immortalized, ACPA-expressing and **B**) tetanus toxoid-specific B cell lines were treated with different doses of acalabrutinib, CCP-Acalabrutinib (CCP-Aca) and CNleP-Acalabrutinib (CNleP-Aca) conjugates for four days in the presence of anti-IgG F(ab')2 antibody fragments from day two on. On day five, XTT viability assay was conducted and the colorimetric result was normalized to the value of anti-IgG- and drug-naive cells (100%). Bars represent the mean of three technical replicates with standard deviation. * $p \leq 0.05$, ** $p \leq 0.01$, *** $p \leq 0.001$, and **** $p \leq 0.0001$ using two-way ANOVA with Tukey's honestly significant difference test. The data shown here are representative of three independent experiments.

The effect of treatment duration on the selective effect of CCP-Acalabrutinib conjugates

Subsequently, we assessed the effect of CCP-Acalabrutinib treatment duration on the viability of both antigen-specific B cell lines. A final concentration of 800 nM Acalabrutinib, CCP-Acalabrutinib and CNleP-Acalabrutinib conjugates were added to both antigen-specific B cell cultures for 2, 3, or 4 consecutive days. Concurrently, anti-IgG stimulation was added to the cultures from day 2

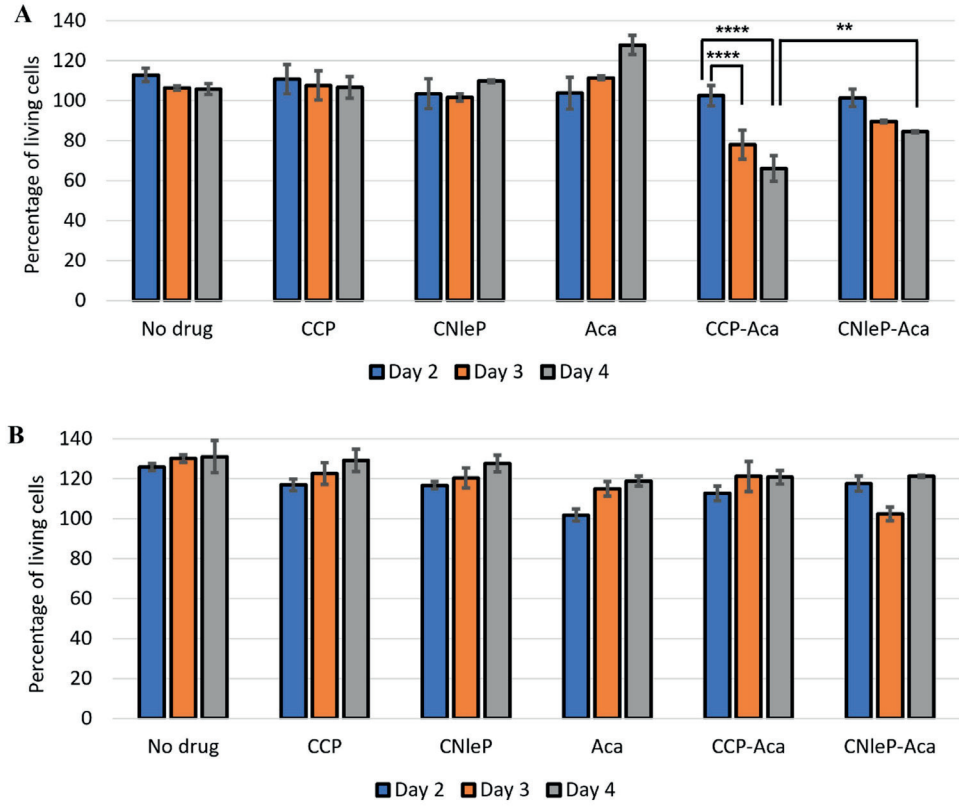

Figure 3. The effect of CCP-acalabrutinib conjugates treatment duration on selective inhibition of ACPA-expressing B cells. A) Immortalized, ACPA-expressing and B) tetanus-toxoid specific B cell lines were treated every day with 800 nM acalabrutinib, CCP, CNleP, CCP-acalabrutinib and CNleP-acalabrutinib conjugates for two, three or four days in the presence of anti-IgG F(ab')2 antibody fragments from day two on. XTT viability assay was performed at day 5and the colorimetric result was normalized to the value of anti-IgG-unstimulated, drug-naive cells (100%). Aca: acalabrutinib. Bar graphs depict the mean of three technical replicates with standard deviation. ** $p \leq 0.01$ and **** $p \leq 0.0001$ using two-way ANOVA with Tukey's honestly significant difference test. The data shown are representative of three independent experiments.

onwards. The day after the last treatment of the cells, an XTT cell viability assay was conducted. Again, we observed a selective effect of CCP-Aca on the viability of ACPA-expressing B cells, which became more prominent with increasing time of culture. As observed previously, CCP-Aca had no consistent effect on the TT-specific control B cell line (Figure 3A and B).

High dose Acalabrutinib alone did not recapitulate the selective effect of CCP-Acalabrutinib

We designed the CCP-Acalabrutinib conjugate to specifically inhibit ACPA-expressing B cells by BCR-mediated endocytosis. Due to this active mechanism, we hypothesized that the concentration of Acalabrutinib inside the cells might by far exceed that of the culture medium. The high intracellular concentration of Acalabrutinib might inhibit not only Btk but also other kinases which leads to reduction of cell viability. If correct, high concentrations of Acalabrutinib should induce an effect similar to a lower concentration of CCP-Acalabrutinib in reducing the viability of ACPA-expressing B cell. Therefore, we next examined whether the selective effect of CCP-Acalabrutinib could be mimicked by high concentrations of Acalabrutinib alone or by a combination of free CCP and free Acalabrutinib. We also extended the treatment duration to six days. In the steady state, the immortalized B cell lines used here require CD40 ligand stimulation and IL-21 for their survival and continuous proliferation.[21] We deliberately removed these stimulants so that CD40 and IL21R signalling pathways did not interfere with the inhibition of BCR signalling. We treated ACPA-expressing and TT-specific B cells for six consecutive days with 800 nM CCP-Acalabrutinib, CNleP-Acalabrutinib conjugates, free peptides, a combination of free peptides and Acalabrutinib, and Acalabrutinib without additional anti-IgG stimulation. In addition, the effect of 4 μM (5 times equivalent) and 8 μM (10 times equivalent) Acalabrutinib on the cell lines was also tested. On day 7, cell viability was measured. We observed that increasing duration of treatment (6 days instead of 5 days) did not enhance the selective effect of CCP-Acalabrutinib on the viability of immortalized, ACPA-expressing B cells (Figure 4). Furthermore, treatment with 8 μM Acalabrutinib or a combination of 800 nM free CCP and Acalabrutinib failed to mimic the effect of 800 nM CCP-Acalabrutinib conjugate on these cells (Figure 4). These findings suggest that the selective effect of CCP-Acalabrutinib on ACPA-expressing B cells requires the presence of CCP in conjugated form and cannot be recapitulated by a ten times higher dose of Acalabrutinib alone.

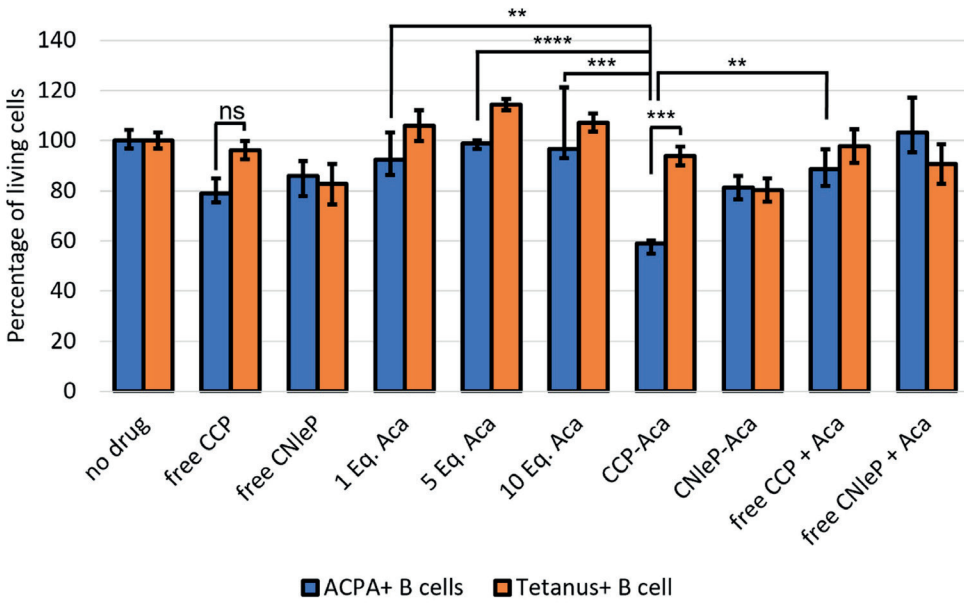

Figure 4. CCP-acalabrutinib conjugation is required for the selective inhibition of ACPA-expressing B cells. Immortalized, ACPA-expressing and tetanus-toxoid specific B cell lines were treated with 800 nM free CCP, free CNleP, CCP-acalabrutinib, CNleP-acalabrutinib conjugates, a combination of free CCP or CNleP with acalabrutinib, acalabrutinib, or 5 and 10 times equivalent (Eq) of acalabrutinib for six consecutive days. On day seven, a XTT viability assay was performed and the colorimetric result was normalized to the value of drug-naive cells (100%). Aca: acalabrutinib. Bar graphs depict the mean of three technical replicates with standard deviation. ** $p \leq 0.01$, *** $p \leq 0.001$, and **** $p \leq 0.0001$ using two-way ANOVA with Tukey's honestly significant difference test. The data are representative of two independent experiments.

CCP-Acalabrutinib affected cell survival in a BCR signalling-independent manner

To investigate the extent of Btk inhibition by CCP-Acalabrutinib conjugates, a competitive activity-based protein profiling assay for Btk was developed. To this end, an activity-based probe in the form of Cy5-labelled Acalabrutinib was synthesized. First, a 5-(4-(2-((tert-butoxycarbonyl)amino)ethyl)piperazin-1-yl)pent-2-ynoic acid handle was conjugated to Acalabrutinib. Then, the tert-butoxycarbonyl protecting group was released by adding hydrochloric acid to yield a reactive amine-containing handle. Subsequently, Cy5-OSu was reacted to the handle-containing Acalabrutinib to generate Cy5-labelled Acalabrutinib (Figure 5). We then treated immortalized, ACPA-expressing and tetanus-toxoid specific B cells with final concentrations of 5 nM, 50 nM and 100 nM of free CCP, Acalabrutinib, and a combination of free CCP and Acalabrutinib, CCP-Acalabrutinib conjugates and CNleP-Acalabrutinib conjugates. After a two-day incubation time, the cells were washed and lysed using lysis buffer. Subsequently, a

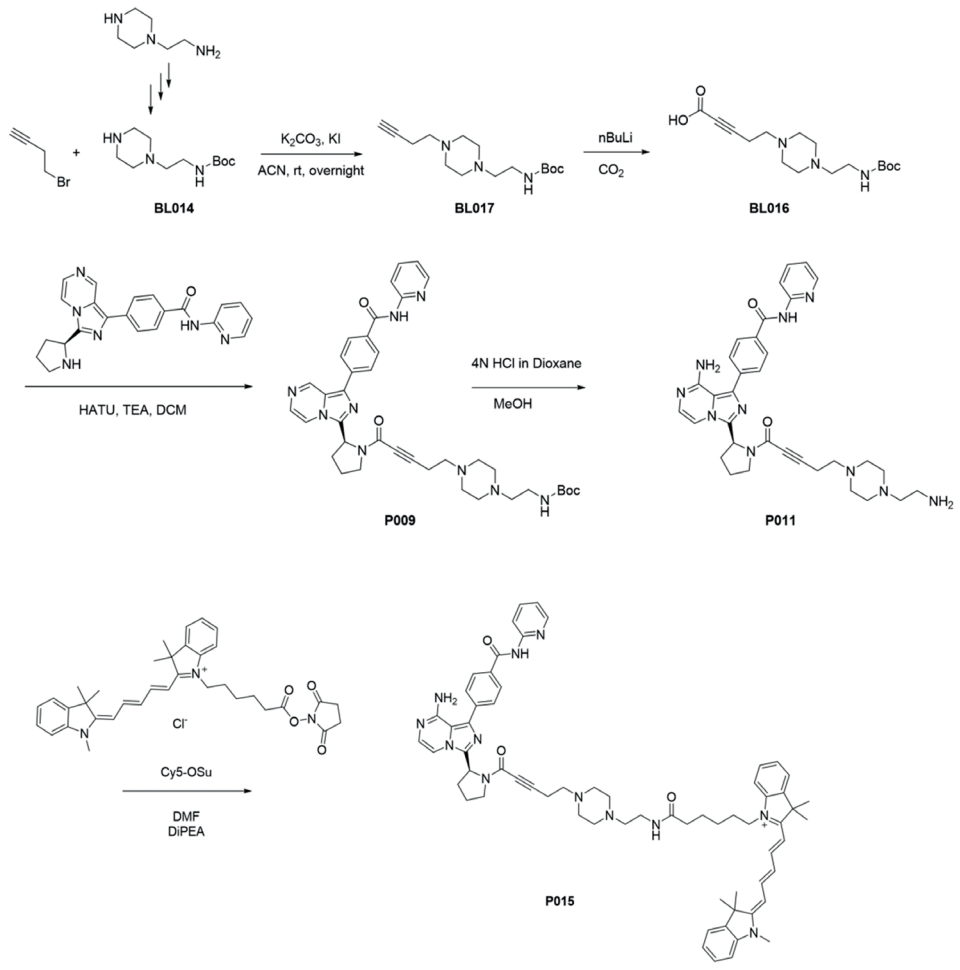

Figure 5. Synthesis of competitive Btk activity-based probe Cy5-labelled Acalabrutinib (P016)

final concentration of 2 μM Cy5-labelled Acalabrutinib was added to the cell lysate at 37°C for 15 minutes where unbound Btk will bind to the probe. The mix was then run on a SDS-polyacrylamide gel and the unbound Btk, the substrate of Cy5-labelled Acalabrutinib, was visualized in-gel with a fluorescence scanner. In this assay, the appearance of a band at the position of the expected Btk molecular weight indicates that Btk is not inhibited during cell treatment. We observed that 5 nM Acalabrutinib already inhibited Btk activity. Furthermore, no band was detected at 100 nM Acalabrutinib-treated cells, indicating full inhibition (Figure 6A). Remarkably, CCP-Acalabrutinib conjugate treatment in any concentration failed to inhibit Btk activity. Similar observations were made for CNleP-Acalabrutinib conjugates (Figure 6A).

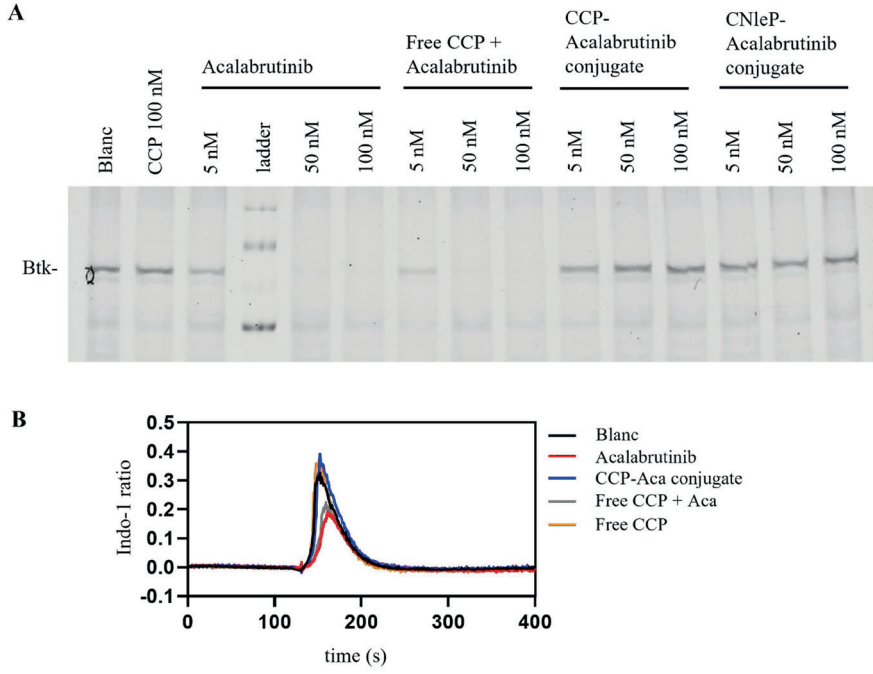

Figure 6. CCP-acalabrutinib conjugates fail to inhibit Btk and BCR signalling. A) Competitive activity-based protein profiling (ABPP) of Btk. Immortalized, ACPA- expressing B cells were treated with the mentioned drug and/or peptide combination at varying doses for two days before being lysed and treated with Cy5-acalabrutinib. The probe-cell lysate mixture was run on SDS/PAGE and visualized by in-gel fluorescence scanning, visualising free Btk binding to the probe. Absence of a fluorescent signal (band) is observed upon complete inhibition of Btk. B) Relative calcium flux intensity (Indo-1 ratio) of drug and/or peptide-treated ACPA-expressing Ramos B cells stimulated with anti-IgG F(ab')2 fragments. A high Indo-1 ratio corresponds to enhanced calcium flux, compatible with BCR signalling-induced B cell activation.

To confirm our findings, we treated ACPA-expressing Ramos B cells with final concentrations of 800 nM Acalabrutinib, free CCP, CCP-Acalabrutinib conjugates and a combination of free CCP and Acalabrutinib for two days.[19] Subsequently, Ca^{2+} flux was measured in these cells upon triggering with anti-IgG F(ab')2 antibody fragments. Ca^{2+} flux is a downstream effect of the BCR signalling pathway. We observed that Acalabrutinib by itself inhibited Ca^{2+} flux (Figure 6B). However, CCP-Acalabrutinib conjugates failed to inhibit this BCR signalling downstream effect (Figure 6B). Together, these findings suggest that CCP-Acalabrutinib conjugates may induce selective effects on ACPA-expressing B cells in our

experimental setting, independent of Btk and BCR signalling inhibition.

Discussion

Aberrant B cells are considered culprits of many forms of leukaemia and autoimmune diseases, including RA. During their development and differentiation, B cells require B cell receptor (BCR) signalling for survival and activation. Therefore, blocking the BCR signalling pathway using Btk inhibitors serves as a promising strategy for therapeutic interventions in B-cell mediated diseases such as RA. Here, we intended to direct Btk-inhibition specifically to auto-reactive B cells. We synthesized Acalabrutinib, a clinically approved second generation Btk inhibitor. Of note, while Acalabrutinib displays Btk-selective kinase inhibition profiles, it still induces adverse side effect in a fraction of leukemic patients.[22] We conjugated this drug to a cyclic citrullinated peptide (CCP) to selectively target ACPA-expressing B cells. We aimed to not only increase the safety profile of Acalabrutinib but also to enhance its efficacy by targeting ACPA-expressing B cells selectively. We hypothesized that CCP conjugation to Acalabrutinib could enhance the enrichment of the drug through BCR-mediated internalization. To test these hypotheses, we used an immortalized, ACPA-expressing B cell line generated previously.

We observed that Acalabrutinib did not reproducibly affect the viability of this immortalized, ACPA-expressing B cell line in the steady state. Also, our control, a tetanus-toxoid specific B cell line, remained unaffected. In line with previous findings, this suggests that BCL-XL and BCL-6 overexpression, the mechanism employed for immortalization of these B cells, alleviates the requirement for active BCR signalling for cell survival. Nonetheless, these cells proliferated when treated with anti-IgG F(ab')2 fragments, suggesting responsiveness to BCR stimulation and BCR-induced proliferation. Consequently, this increase could indeed be suppressed by treatment with Acalabrutinib. Notably, CCP-Acalabrutinib conjugates also showed this effect, but additionally suppressed the viability of the immortalized, ACPA-expressing B cell line in a dose and time dependent manner. Moreover, this additional inhibitory effect was not observed in the tetanus-toxoid specific control B cell line. While the mechanism underlying this CCP-conjugate dependent effect remains uncertain, these findings would be compatible with a selective, yet Btk-inhibition independent, cytotoxic effect of CCP-Acalabrutinib conjugates on ACPA-expressing B cells.

Based on the observations described, we intended to investigate whether CCP-Acalabrutinib conjugates indeed inhibited Btk. Using an ABPP assay, we showed

that 100 nM Acalabrutinib readily inhibited Btk completely. At this concentration of CCP-Acalabrutinib, however, Btk was not inhibited. This finding was confirmed by the failure of CCP-Acalabrutinib conjugates to inhibit anti-IgG-induced calcium flux. Nonetheless, the effect of CCP-Acalabrutinib conjugates intensified with increasing doses higher than 100 nM suggesting that the conjugates exert their effects by inhibiting off-target tyrosine kinases outside the BCR signalling pathway.[23] As 4 μM and 8 μM of Acalabrutinib failed to mimic the effects of 800 nM CCP-Acalabrutinib conjugates, it is possible that Acalabrutinib binding to off-target kinases requires co-localization with the BCR to exert this effect. Importantly, a combination of free CCP and free Acalabrutinib did not induce similar effects. As CCP-Acalabrutinib failed to inhibit Btk in the ABPP assay, it is likely that the conjugates did not diffuse into the cytosolic compartment where Btk is located. One possible explanation could be that while CCP monomers may bind cell surface BCRs, they may not be able to cross-link BCR molecules, thereby failing to induce BCR signalling and internalization. Whether CCP-Acalabrutinib conjugates are internalized via different routes, or whether Acalabrutinib may bind to cell surface molecules in the vicinity of ACPA-BCRs and thereby exert the effect observed, remains to be determined. One of the off-target receptor tyrosine kinases of Acalabrutinib is epithelial growth factor receptor (EGFR). Pull down experiments of CCP-Acalabrutinib binding proteins may give insights into possible off-target protein binding of the conjugates, which will be important to elucidate prior to the use of antigen-Acalabrutinib conjugates in a clinical setting. In addition, similar experiments using CCP-dimers or polymers conjugated to Acalabrutinib together with studies on the internalization of the conjugates may help to dissect Btk-dependent and -independent effects.

In conclusion, in the experiments presented, CCP-Acalabrutinib conjugates showed selective inhibitory effects on ACPA-expressing B cells in a Btk inhibition-independent manner. Efforts to pinpoint the targets of CCP-Acalabrutinib may support the development of highly specific targeting strategies for autoreactive B cells, which will be relevant for novel therapeutic interventions in RA and other autoimmune diseases.

Reference

1. Kristyanto H, Blomberg NJ, Slot LM, et al. Persistently activated, proliferative memory autoreactive B cells promote inflammation in rheumatoid arthritis. *Science translational medicine* 2020; **12**(570).

2. Fujimoto M, Poe JC, Satterthwaite AB, Wahl MI, Witte ON, Tedder TF. Complementary roles for CD19 and Bruton's tyrosine kinase in B lymphocyte signal transduction. *Journal of immunology (Baltimore, Md : 1950)* 2002; **168**(11): 5465-76.

3. Taylor DK, Ito E, Thorn M, Sundar K, Tedder T, Spatz LA. Loss of tolerance of anti-dsDNA B cells in mice overexpressing CD19. *Molecular immunology* 2006; **43**(11): 1776-90.

4. Sato S, Fujimoto M, Hasegawa M, Takehara K, Tedder TF. Altered B lymphocyte function induces systemic autoimmunity in systemic sclerosis. *Molecular immunology* 2004; **41**(12): 1123-33.

5. Corneth OBJ, Verstappen GMP, Paulissen SMJ, et al. Enhanced Bruton's Tyrosine Kinase Activity in Peripheral Blood B Lymphocytes From Patients With Autoimmune Disease. *Arthritis & rheumatology (Hoboken, NJ)* 2017; **69**(6): 1313-24.

6. Wu H, Huang Q, Qi Z, et al. Irreversible inhibition of BTK kinase by a novel highly selective inhibitor CHMFL-BTK-11 suppresses inflammatory response in rheumatoid arthritis model. *Scientific reports* 2017; **7**(1): 466.

7. Haselmayer P, Camps M, Liu-Bujalski L, et al. Efficacy and Pharmacodynamic Modeling of the BTK Inhibitor Evobrutinib in Autoimmune Disease Models. *Journal of immunology (Baltimore, Md : 1950)* 2019; **202**(10): 2888-906.

8. Woyach JA, Johnson AJ, Byrd JC. The B-cell receptor signaling pathway as a therapeutic target in CLL. *Blood* 2012; **120**(6): 1175-84.

9. Byrd JC, Hillmen P, O'Brien S, et al. Long-term follow-up of the RESONATE phase 3 trial of ibrutinib vs ofatumumab. *Blood* 2019; **133**(19): 2031-42.

10. Long M, Beckwith K, Do P, et al. Ibrutinib treatment improves T cell number and function in CLL patients. *The Journal of clinical investigation* 2017; **127**(8): 3052-64.

11. Dickerson T, Wiczer T, Waller A, et al. Hypertension and incident cardiovascular events following ibrutinib initiation. *Blood* 2019; **134**(22): 1919-28.

12. Ezad S, Khan AA, Cheema H, et al. Ibrutinib-related atrial fibrillation: A single center Australian experience. *Asia-Pacific journal of clinical oncology* 2019;

15(5): e187-e90.

13. Awan FT, Schuh A, Brown JR, et al. Acalabrutinib monotherapy in patients with chronic lymphocytic leukemia who are intolerant to ibrutinib. *Blood advances* 2019; **3**(9): 1553-62.

14. Podoll T, Pearson PG, Evarts J, et al. Bioavailability, Biotransformation, and Excretion of the Covalent Bruton Tyrosine Kinase Inhibitor Acalabrutinib in Rats, Dogs, and Humans. *Drug metabolism and disposition: the biological fate of chemicals* 2019; **47**(2): 145-54.

15. Owen RG, McCarthy H, Rule S, et al. Acalabrutinib monotherapy in patients with Waldenström macroglobulinemia: a single-arm, multicentre, phase 2 study. *The Lancet Haematology* 2020; **7**(2): e112-e21.

16. Fulmer GR, Miller AJM, Sherden NH, et al. NMR Chemical Shifts of Trace Impurities: Common Laboratory Solvents, Organics, and Gases in Deuterated Solvents Relevant to the Organometallic Chemist. *Organometallics* 2010; **29**(9): 2176-9.

17. Lelieveldt L, Kristyanto H, Pruijn GJM, Scherer HU, Toes REM, Bonger KM. Sequential Prodrug Strategy To Target and Eliminate ACPA-Selective Autoreactive B Cells. *Mol Pharm* 2018; **15**(12): 5565-73.

18. Kristyanto H, Holborough-Kerkvliet MD, Lelieveldt L, et al. Multifunctional, Multivalent PIC Polymer Scaffolds for Targeting Antigen-Specific, Autoreactive B Cells. *ACS Biomater Sci Eng* 2022; **8**(4): 1486-93.

19. Kissel T, Reijm S, Slot LM, et al. Antibodies and B cells recognising citrullinated proteins display a broad cross-reactivity towards other post-translational modifications. *Annals of the rheumatic diseases* 2020; **79**(4): 472-80.

20. Kissel T, Ge C, Hafkenscheid L, et al. Surface Ig variable domain glycosylation affects autoantigen binding and acts as threshold for human autoreactive B cell activation. *Sci Adv* 2022; **8**(6): eabm1759.

21. Kwakkenbos MJ, Diehl SA, Yasuda E, et al. Generation of stable monoclonal antibody–producing B cell receptor–positive human memory B cells by genetic programming. *Nature medicine* 2010; **16**(1): 123-8.

22. Sharman JP, Egyed M, Jurczak W, et al. Acalabrutinib with or without obinutuzumab versus chlorambucil and obinutuzmab for treatment-naive chronic lymphocytic leukaemia (ELEVATE TN): a randomised, controlled, phase 3 trial. *Lancet* 2020; **395**(10232): 1278-91.

23. Byrd JC, Harrington B, O'Brien S, et al. Acalabrutinib (ACP-196) in Relapsed Chronic Lymphocytic Leukemia. 2015; **374**(4): 323-32.